

Supporting Information

Contents of this file

Text S1

Figure S1

Test S1

High spatial resolution of the GEONET dense array of GPS receivers provided the powerful opportunity to observe the evolution of STIDs following the 2011 Tohoku earthquake previously [1-5]. In this study, the GEONET/TEC data of ~1200 receivers are employed again to verify the reliability of F3/C RO observations. Methods to resolve ground-based GPS TEC have been introduced in detail in plentiful studies (e.g., [1, 6] and references therein). In short, the slant TEC can be measured from the trans-ionospheric signals recorded at ground-based GPS receivers by means of calculating the difference between the P1/P2 pseudoranges and the combination of the phases at two carrier signals (L1/L2). The vertical TEC, then, can be calculated based on a thin shell approximation [7]. The ionosphere is assumed to be concentrated at a height of 300 km, and a sub ionospheric point (SIP) is the projection of an ionospheric piercing point to the Earth's surface under the thin shell assumption. To degrade the multipath effect, we use only data with elevations higher than 20°. The ionospheric perturbations are extracted from the resolved TEC series using four-order zero phase shift Butterworth filter with a lower cutoff period of 1 min and a higher cutoff period of 15 min [8]. In Figure 8a of the manuscript, the locations of the ~1200 ground-based GPS receivers are shown as black triangles, and the traces of sub ionospheric points (SIPs) for satellites 5, 9, 15, 18, 21, 22, 26, and 27 during the period of 5.5–9.0 UT are shown as green curves.

Figure S1 denotes the travel-time diagram of ionospheric TEC perturbations as a function of distance from the epicenter (0-4000 km) and universal time (5.5 -9.0 UT) derived from ground-based GPS observations with PRN 5, 9, 15, 18, 21, 22, 26, and 27, respectively. The concept of "travel time" originated from seismology can be used to extract the propagation speed of different types of waves. Remarkable STIDs are observed moving away from the epicenter at approximate apparent velocity of 3000 m/s, 500-800 m/s and 100–300 m/s, consistent with Rayleigh waves, acoustic waves, and gravity waves, respectively. To be specific, we observe an acoustic wave coupled with Rayleigh wave (AWRayleigh) starting from the epicenter with a speed of around 3.0 km/s. Another type of STIDs (AGWepi) occurs within ~60 minutes after the earthquake, and can be clearly divided into two components: a faster (~500-800 m/s) acoustic wave mode and a slower (~200-300 m/s) gravity wave mode. They are generated at the epicenter by the rupture of the crust and gradually attenuated ~800 km away. Then, they are replaced by a gravity wave coupled with the tsunami (IGWtsunami) that moves with an apparent speed of between 100 and 300 m/s. The above results agree with previous studies using ground-based GPS receiving networks [1-4].

Tracks of the selected three F3/C measurements (Figure 8a) cover the far field areas, which compensate for the limitation of the ground-based GPS observations. In Figure S1, the profiles P1, P2 and P3 from the satellite-based GPS TEC surveys are superimposed on the ground-based GPS TEC observations. The scatter dots of the three profiles (the tangent points of which are shown in Figure 8a), represent the detrended F3/C TEC during the RO sounding period. It can be clearly seen that the time of the F3/C TEC perturbations depended on the propagation distance is consistent with the ground-based GPS TEC observations. It indicates that during the movement of the horizontal projection trajectory of the occultation tangent point, the tangent point passes through the positive and negative phases of the acoustic-gravity waves in the ionosphere. It should be noted that due to the difference observing geometry between

ground-based and satellite-based GPS, the amplitude and wavelength of the TEC perturbations extracted by the two measurements are not comparable, resulting in the amplitude recorded by P1, P2 and P3 profiles in the traveling time diagram is much larger than the color scale. Exactly, the ground-based GPS receivers probed the STIDs during 4.5-hour period, while the F3/C took few minutes to finish a RO detection. While the amplitude of a perturbation is different from ground-based TEC and F3/C TEC, the time of arrival and the velocity can still be compared with each other.

Figure S1

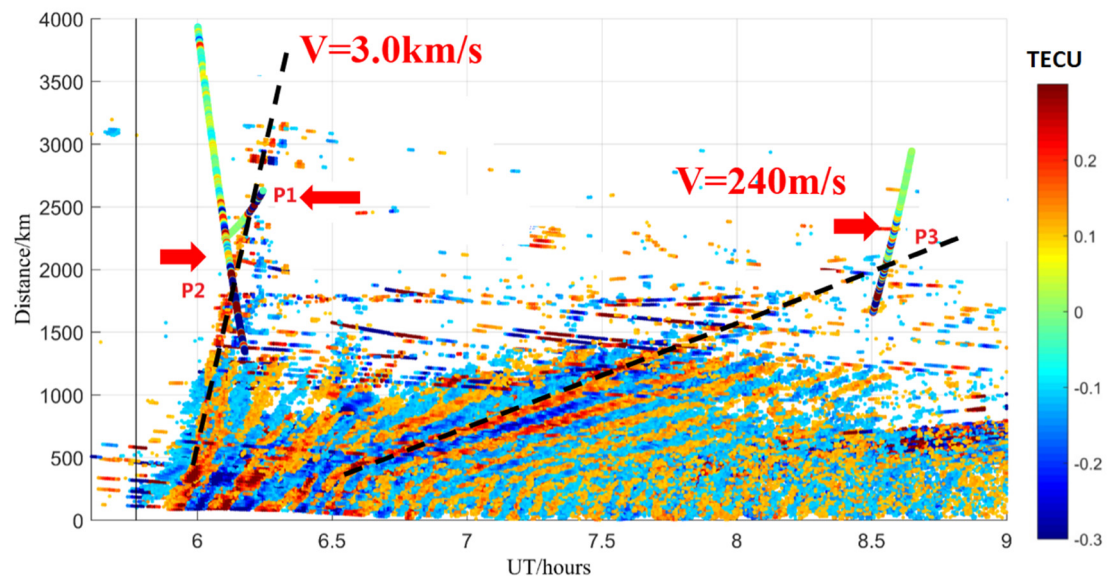


Figure S1. Traveling time diagram of the TEC perturbation data following the Tohoku earthquake. The color of the scatters represents the amplitude of the TEC perturbation. Scattered dots named P1, P2 and P3 show the F3/C detrended TEC profiles. The black dashed lines are used to fit the propagation velocities of the STIDs. The vertical black line indicates the onset time of the earthquake.

Acknowledgments: The F3/C RO data are obtained by the COSMIC Data Analysis Archive Center (CDAAC) (<http://cdaac-www.cosmic.ucar.edu/cdaac/index.html>). The ground-based GPS data are obtained from the Geospatial Information Authority of Japan (GSI).

References.

- Galvan, D.A.; Komjathy, A.; Hickey, M.P.; Stephens, P.; Snively, J.; Tony Song, Y.; Butala, M.D.; Mannucci, A.J. Ionospheric signatures of Tohoku-Oki tsunami of March 11, 2011: Model comparisons near the epicenter. *Radio Sci.* **2012**, *47*.
- Jin, S.; Jin, R.; Li, J.H. Pattern and evolution of seismo-ionospheric disturbances following the 2011 Tohoku earthquakes from GPS observations. *J. Geophys. Res. Sp. Phys.* **2014**, *119*, 7914–7927.
- Rolland, L.M.; Lognonné, P.; Astafyeva, E.; Kherani, E.A.; Kobayashi, N.; Mann, M.; Munekane, H. The resonant response of the ionosphere imaged after the 2011 off the Pacific coast of Tohoku Earthquake. *Earth, Planets Sp.* **2011**, *63*, 853–857.
- Occhipinti, G.; Rolland, L.; Lognonné, P.; Watada, S. From Sumatra 2004 to Tohoku-Oki 2011: The systematic GPS detection of the ionospheric signature induced by tsunamigenic earthquakes. *J. Geophys. Res. Sp. Phys.* **2013**, *118*, 3626–3636.
- Astafyeva, E.; Lognonné, P.; Rolland, L. First ionospheric images of the seismic fault slip on the example of the Tohoku-oki earthquake. *Geophys. Res. Lett.* **2011**, *38*, 1–6.
- Heki, K.; Ping, J. Directivity and apparent velocity of the coseismic ionospheric disturbances observed with a dense GPS array. *Earth Planet. Sci. Lett.* **2005**, *236*, 845–855.

7. Klobuchar, J.A. Ionospheric Time-Delay Algorithm for Single-Frequency GPS Users. *IEEE Trans. Aerosp. Electron. Syst.* **1987**, AES-23, 325–331
8. Makela, J.J.; Lognonné, P.; Hébert, H.; Gehrels, T.; Rolland, L.; Allgeyer, S.; Kherani, A.; Occhipinti, G.; Astafyeva, E.; Cosson, P.; et al. Imaging and modeling the ionospheric airglow response over Hawaii to the tsunami generated by the Tohoku earthquake of 11 March 2011. *Geophys. Res. Lett.* **2011**, *38*.